Colistin kills bacteria by targeting lipopolysaccharide in the cytoplasmic membrane

Akshay Sabnis[1], Katheryn L. H. Hagart[1], Anna Klöckner[1,2,3], Michele Becce[3], Lindsay E. Evans[1,4], R. Christopher D. Furniss[1], Despoina A. I. Mavridou[5], Ronan Murphy[6,7], Molly M. Stevens[2,3], Jane C. Davies[6,7], Gerald J. Larrouy-Maumus[1], Thomas B. Clarke[1] and Andrew M. Edwards[1#]

[1] MRC Centre for Molecular Bacteriology and Infection, Imperial College London, Armstrong Rd., London, SW7 2AZ, UK.

[2] Department of Bioengineering, Imperial College London, Imperial College London Rd., London, SW7 2AZ, UK.

[3] Department of Materials, Imperial College London, Imperial College London Rd., London, SW7 2AZ, UK.

[4] Department of Chemistry, Imperial College London, Molecular Sciences Research Hub, White City Campus, Wood Lane, London, W12 OBZ, UK.

[5] Department of Molecular Biosciences, University of Texas at Austin, Austin, 78712, Texas, USA.

[6] National Heart and Lung Institute, Imperial College London, Imperial College London Rd., London, SW7 2AZ, UK.

[7] Department of Paediatric Respiratory Medicine, Royal Brompton Hospital, Sydney Street, London, SW3 6NP, UK.

[#] For correspondence:
Tel: 0044 (0)207 594 2072
Fax: 0044 (0)207 594 3096
a.edwards@imperial.ac.uk

Keywords: Colistin / polymyxin / *Pseudomonas* / *E. coli* / *Klebsiella* / lipopolysaccharide / resistance / MCR-1

Running title: Colistin mechanism of action

Summary

Colistin is an antibiotic of last resort, but has poor efficacy and resistance is a growing problem. Whilst it is well established that colistin disrupts the bacterial outer membrane by selectively targeting lipopolysaccharide (LPS), it was unclear how this led to bacterial killing. We discovered that MCR-1 mediated colistin resistance is due to modified LPS at the cytoplasmic rather than outer membrane. In doing so, we also demonstrated that colistin exerts bactericidal activity by targeting LPS in the cytoplasmic membrane. We then exploited this information to devise a new therapeutic approach. Using the LPS transport inhibitor murepavadin, we were able to cause LPS accumulation in the cytoplasmic membrane, which resulted in increased susceptibility to colistin *in vitro* and improved treatment efficacy *in vivo*. These findings reveal new insight into the mechanism by which colistin kills bacteria, providing the foundations for novel approaches to enhance therapeutic outcomes.

62 **Introduction**

63 The emergence of multi-drug-resistant Gram-negative pathogens such as *Escherichia coli*, *Klebsiella*
64 *pneumoniae* and *Pseudomonas aeruginosa* has led to the increased use of polymyxin antibiotics, which are
65 often the only viable last-resort therapeutic option [1-4]. Two closely related polymyxin antibiotics are used
66 clinically, colistin (polymyxin E) and polymyxin B, which share a high degree of structural similarity, consisting
67 of a cationic peptide ring of 7 amino acids connected to a hydrophobic acyl tail by a linear chain of 3 amino
68 acids [1,3].

69 Polymyxins are rapidly bactericidal towards Gram-negative bacteria *in vitro* but are considerably less
70 efficacious *in vivo*, with up to 70% of patients failing to respond to colistin treatment [5-7]. Restrictions on
71 dosage due to the nephrotoxicity of polymyxins means that only 50% of people with normal renal function
72 achieve a steady state serum concentration sufficient to kill bacteria [8,9]. As such, there is a desperate need
73 to develop new approaches to enhance the efficacy of polymyxin antibiotics.

74 Barriers to increasing polymyxin efficacy include the significant gaps in our understanding of their mode of
75 action. Whilst it is well established that the binding of polymyxins to LPS on the surface of Gram-negative
76 bacteria leads to disruption of the outer membrane (OM), it is unclear how this results in cell lysis and
77 bacterial death (Supplementary Fig. 1) [3,10]. It is hypothesised that damage to the LPS monolayer enables
78 polymyxins to traverse the OM via a process of 'self-directed uptake', although this has not been
79 demonstrated experimentally [10,11]. Once across the OM, polymyxins permeabilize the cytoplasmic
80 membrane (CM), which is required for bacterial lysis and killing [1-3]. However, the mechanism by which
81 colistin damages the CM is unclear [11,12]. It has been proposed that the surfactant activity of polymyxins,
82 conferred by the positively charged peptide ring and hydrophobic tail, is sufficient to compromise the
83 phospholipid bilayer of the CM via a detergent-like effect [1,3]. In support of this, polymyxins can interact
84 with mammalian cell membranes, leading to changes in epithelial monolayer permeability [13]. Polymyxin
85 antibiotics also have some inhibitory activity against the Gram-positive bacterium *Streptococcus pyogenes*,
86 where the CM is formed of a phospholipid bilayer [14].

87 However, several lines of evidence call into doubt the ability of physiologically relevant concentrations of
88 polymyxins to disrupt phospholipid bilayers. Firstly, the concentrations of polymyxin B required to disrupt
89 mammalian epithelial cells or inhibit the growth of *S. pyogenes* (8-16 μg ml^{-1}) are above typical serum
90 concentrations of the antibiotic, and colistin at clinically-relevant concentrations displays no activity against
91 other Gram-positive organisms such as *Staphylococcus aureus* and *Enterococcus faecalis* [13-16].
92 Furthermore, colistin has very little activity against synthetic phospholipid bilayer membranes unless LPS is
93 present, a finding that explains why polymyxins are 30-100-fold less active against colistin-resistant *A.*
94 *baumanii* isolates that are LPS-deficient, with an OM composed of a phospholipid bilayer [17-19]. Finally,
95 molecular dynamics simulations show that the interaction of colistin with phospholipid bilayers is unlike what

has been reported for other antimicrobial peptides that target phospholipid bilayers [20]. Together, these observations call into question whether, at physiologically relevant concentrations, colistin disrupts the CM of Gram-negative bacteria via the engagement of the polymyxin antibiotic with membrane phospholipids.

In addition to the mode of action of colistin, there are also gaps in our understanding of the mechanisms by which colistin resistance protects bacteria from polymyxin antibiotics. In Gram-negative bacteria, LPS is synthesised in the cytoplasm via the Raetz pathway, during which it is introduced into the inner leaflet of the CM [26,27]. It is then flipped to the outer leaflet of the CM by MsbA before transportation to the OM via the LptABCDEFG machinery [28-30]. To date, 10 mobile colistin resistance (*mcr*) gene variants have been described, all of which encode phosphoethanolamine (pEtN) transferases that modify the lipid A component of LPS with pEtN as it is trafficked through the CM on the way to the OM [21-25]. Colistin resistance can also arise via mutations in genes encoding two-component regulatory systems such as PhoPQ, PmrAB or BasRS [31,32]. This typically leads to the addition of 4-amino-4-deoxy-l-arabinose (L-ara4N) and/or pEtN groups to LPS, with this modification also occurring at the CM [27,31].

Despite the association between MCR-mediated LPS modification and colistin resistance, there is evidence that it does not prevent polymyxin-mediated damage of the OM. For example, colistin has been shown to permit ingress of the *N*-phenyl-1-napthylamine (NPN) fluorophore into the OM of *E. coli* expressing *mcr*-1 [10]. Furthermore, colistin greatly enhances the activity of hydrophobic antibiotics such as rifampicin against polymyxin-resistant bacteria via disruption of the OM [33]. However, despite colistin damaging the OM of resistant bacteria, it is unable to kill or lyse them [10]. This suggests that the modification of LPS with pEtN and/or L-ara4N protects the CM from colistin, but it is not clear how [10,33].

Improving our knowledge of how colistin kills bacteria is essential to help devise new approaches to enhance the efficacy of last resort polymyxin antibiotics [21-25]. To do this, we set out to better understand how *mcr*-1 protects bacteria from colistin and to then use this information to elucidate the mode of action of colistin, with the ultimate aim of exploiting this information to improve colistin efficacy.

127 **Results**

128 **MCR-1 protects the CM but not the OM from colistin-mediated disruption**

129 The first issue we wanted to resolve was whether MCR-1 protected the CM and/or OM of bacteria from
130 colistin. To do this, we used an isogenic *E. coli* MC1000 strain pair, one of which expresses *mcr*-1 from the
131 IPTG-inducible vector pDM1 (*mcr*-1) to ensure consistent expression under our experimental conditions, and
132 the other transformed with the pDM1 vector alone as a control (pEmpty) [34]. As expected, we found that *E.*
133 *coli* MC1000 expressing *mcr-1* had a significantly greater colistin minimum inhibitory concentration (MIC, 2
134 µg ml^{-1}) compared to the MC1000 pEmpty control strain (0.25 µg ml^{-1}), which was similar to that seen for
135 clinical isolates [34] (Supplementary Fig. 2). This confirmed that the *E. coli* cells were producing functional
136 MCR-1.

137 To fully characterise the LPS-modifying activity of MCR-1, we undertook MALDI-TOF-based lipidomic analysis
138 of both whole *E. coli* cells and *E. coli* spheroplasts that lacked an OM [35]. We confirmed spheroplast
139 formation by microscopy and used FITC labelling of OM surface proteins to demonstrate removal of the OM
140 (Supplementary Fig. 3, 4). Our lipidomic analysis revealed the presence of LPS modified with pEtN in both the
141 CM and OM of *mcr*-1 expressing bacteria, consistent with the location of MCR-1 in the CM [34,36]
142 (Supplementary Fig. 5). Of note, whilst 42±19% of total cellular LPS from MCR-1-producing *E. coli* was
143 unmodified, the proportion of unmodified LPS in the CM was just 21±2% (Fig. 1A, Supplementary Fig. 5).

144 We next assessed the effect of colistin on the integrity of the *E. coli* OM using the hydrophobic NPN dye,
145 which fluoresces upon contact with phospholipids exposed by damage to the LPS monolayer [10,37]. As
146 expected, colistin caused permeabilization of the OM of the *E. coli* pEmpty strain in a dose-dependent
147 manner (Fig. 1B). In agreement with previous findings, we found that colistin also disrupted the OM of *E. coli*
148 expressing *mcr*-1 to a similar degree to *E. coli* pEmpty (Fig. 1B) [10]. Therefore, MCR-1-mediated changes to
149 LPS did not prevent permeabilization of the OM by colistin, which reflects the presence of the relatively large
150 quantity of unmodified LPS in the OM as determined in our lipidomic analysis (Fig. 1A, Supplementary Fig. 5).

151 Next, we assessed damage to the CM structure in the *E. coli* strain pair during colistin exposure, using the
152 membrane impermeant dye propidium iodide (PI). PI fluoresces upon contact with DNA in the bacterial
153 cytoplasm, and thus is indicative of permeabilization of the both the OM and CM of whole bacterial cells
154 [38,39]. As expected, colistin exposure resulted in a strong PI signal from *E. coli* pEmpty cells, indicative of
155 CM permeabilization (Fig. 1C). However, despite colistin permeabilizing the OM of *E. coli* expressing *mcr*-1,
156 the CM of these bacteria remained intact, as demonstrated by the lack of PI-mediated fluorescence (Fig. 1C).
157 In keeping with these findings, colistin caused lysis of *E. coli* pEmpty cells, as seen by a reduction in OD_{595nm}
158 readings over time (Fig. 1D). By contrast, *E. coli* cells producing MCR-1 grew in the presence of colistin despite
159 the damage the polymyxin caused to the OM, as demonstrated by an increase in OD_{595nm} measurements over

160 time (Fig. 1D). Taken together, these data demonstrate that MCR-1 protects the CM but not the OM from
161 colistin.

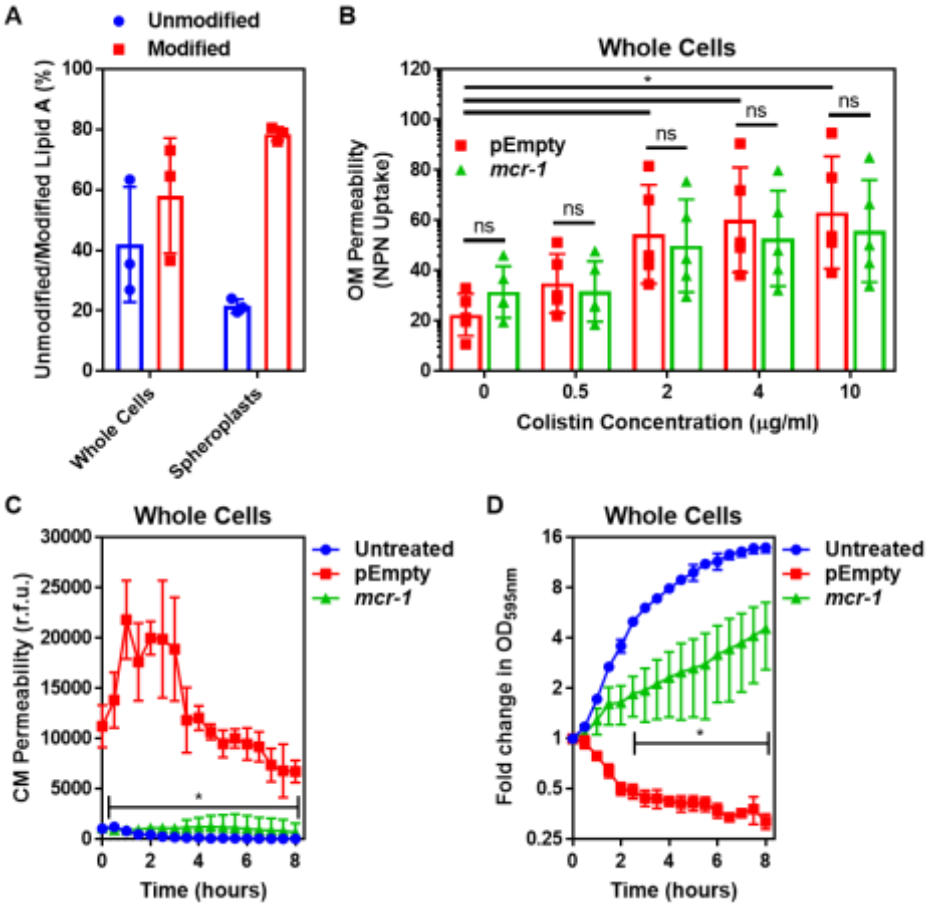

162

163 **Figure 1. Colistin disrupts the outer membrane but not the cytoplasmic membrane of *E. coli* expressing *mcr-1*. A,**
164 Quantification of LPS modified with phosphoethanolamine, expressed as the percentage of unmodified lipid A and
165 unmodified lipid A, in whole cells and spheroplasts of E. coli MC1000 expressing *mcr-1*, as determined by MALDI-TOF-
166 based lipidomics (n=3 in duplicate, *p<0.05 between Whole Cells and Spheroplasts). **B,** OM disruption of *E. coli* MC1000
167 cells expressing *mcr-1* or an empty plasmid control strain (pEmpty) during 10 minutes of exposure to colistin at the
168 indicated antibiotic concentrations, as determined by uptake of the fluorescent dye NPN (10 µM) (n=5, each data point
169 represents the arithmetic mean of 20 replicate measurements; ns: p>0.05 between pEmpty and *mcr-1* strains, *p<0.05
170 between the indicated concentrations of colistin). **C,** Permeabilization of the CM of *E. coli* MC1000 cells expressing *mcr-*
171 *1* or empty plasmid-containing cells during incubation with colistin (4 µg ml^{-1}), as determined using 2.5 µM propidium
172 iodide (PI) (n=4; *p<0.0001 between pEmpty and *mcr-1* strains). **D,** Growth or lysis of *E. coli* MC1000 cells expressing
173 *mcr-1* or empty plasmid control cells during exposure to colistin (4 µg ml^{-1}), as measured using OD_{595nm} readings (n=4;
174 *p<0.05 between pEmpty and *mcr-1* strains). Data in **A** were analysed by a two-tailed paired Student's t-test. Data in **B-**
175 **D** were analysed by a two-way ANOVA with Sidak's **(B)** or Dunnett's **(C,D)** post-hoc tests. Data are presented as the
176 arithmetic mean, and error bars represent the standard deviation of the mean. OM: outer membrane; NPN: *N*-phenyl-
177 1-naphthylamine; CM: cytoplasmic membrane; r.f.u.: relative fluorescence units; OD: optical density.
178

179 **Colistin targets LPS in the CM**

180 To explain the ability of MCR-1-mediated LPS modification to protect the CM from colistin, we considered
181 two possibilities. Firstly, that LPS modifications alter the biophysical properties of the phospholipid bilayer of
182 the CM [10]. Secondly, that colistin targets LPS in the CM and that modification with pEtN confers protection.

183 To test the first possibility, we determined the susceptibility of spheroplasts from *E. coli* MC1000 *mcr*-1 or
184 pEmpty to colistin or the cationic antimicrobial peptides (CAMPs) daptomycin or nisin. Both CAMPs are well
185 characterised for their ability to permeabilize phospholipid bilayers and, like colistin, they are positively
186 charged, enabling us to detect whether any changes to membrane charge or fluidity conferred by MCR-1-
187 modified LPS in the CM contributed to polymyxin resistance [40,41].

188 The CM of spheroplasts of *E. coli* MC1000 *mcr*-1 was resistant to damage by colistin, but susceptible to
189 daptomycin and nisin (Fig. 2A,B,C). By contrast, colistin, daptomycin and nisin all permeabilized the CM of
190 spheroplasts of *E. coli* pEmpty (Fig. 2A,B,C). In keeping with the data from assays measuring CM damage,
191 colistin, daptomycin and nisin all caused lysis of spheroplasts of *E. coli* pEmpty, whilst the spheroplasts from
192 *E. coli* expressing *mcr-1* were undamaged by colistin, but were lysed by both daptomycin and nisin (Fig.
193 2D,E,F). Combined, these data demonstrated that the protection afforded to the CM by MCR-1 is specific for
194 colistin, and that that the polymyxin antibiotic does not share the same target as the phospholipid-targeting
195 CAMPs. Thus, since MCR-1 specifically modifies LPS and selectively protects the CM from colistin, we
196 concluded that LPS is the CM target of colistin, just as it is in the OM.

197

198

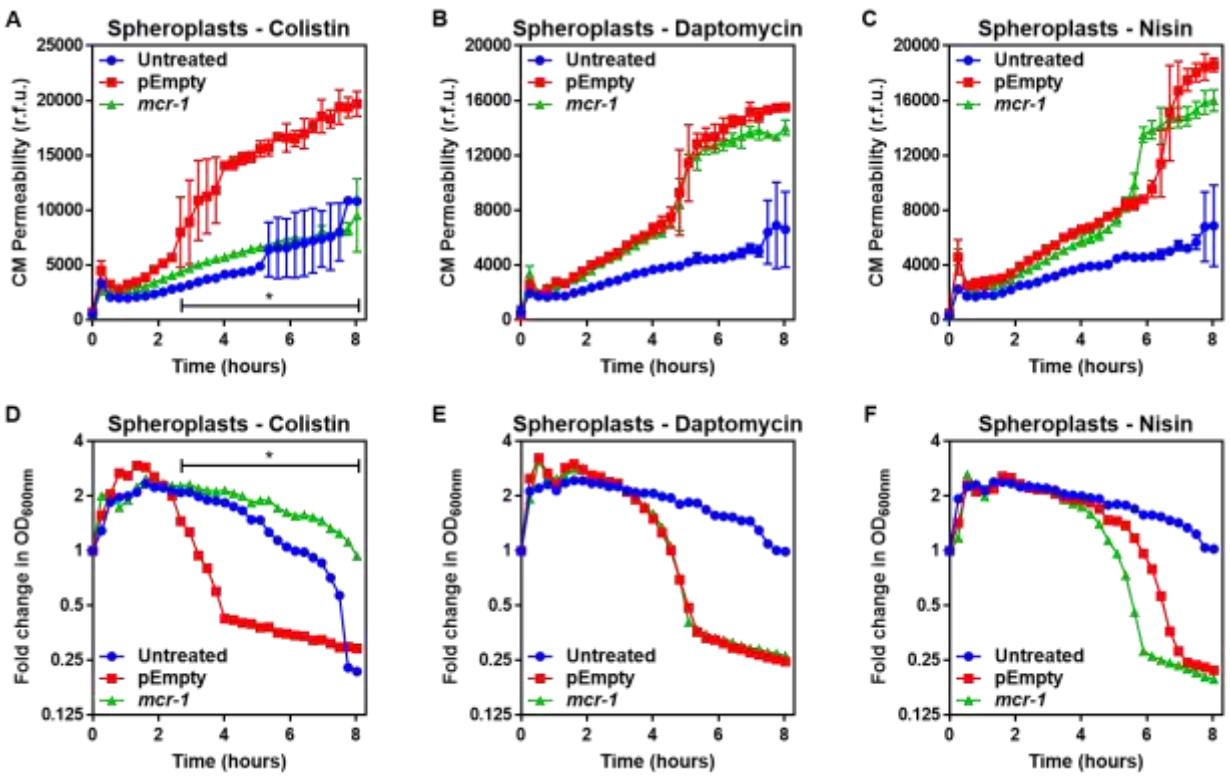

Figure 2. MCR-1 protects the cytoplasmic membrane of *E. coli* spheroplasts from colistin but not other cationic antimicrobial peptides. A-C, Permeabilization of the CM of *E. coli* MC1000 spheroplasts generated from bacteria expressing *mcr-1* or empty plasmid control bacteria (pEmpty) during incubation with **(A)** colistin (4 µg ml^{-1}), **(B)** daptomycin (20 µg ml^{-1}, with 1.25 µM Ca^{2+} ions) or **(C)** nisin (20 µg ml^{-1}), as determined using 0.25 µM PI (n=3, experiment performed on 4 independent occasions; *p<0.01 between pEmpty and *mcr-1* strains). **D-F,** Lysis of *E. coli* MC1000 spheroplasts generated from bacteria expressing *mcr-1* or empty plasmid control bacteria during incubation with **(D)** colistin (4 µg ml^{-1}), **(E)** daptomycin (20 µg ml^{-1}, with 1.25 µM Ca^{2+} ions) or **(F)** nisin (20 µg ml^{-1}), as measured using OD_{600nm} readings (n=3, experiment performed on 4 independent occasions; *p<0.05 between pEmpty and *mcr-1* strains, error bars are omitted for clarity). Data in **A-F** were analysed by a two-way ANOVA with Dunnett's post-hoc test. Data are presented as the arithmetic mean, and error bars, where shown, represent the standard deviation of the mean. CM: cytoplasmic membrane; r.f.u.: relative fluorescence units; OD: optical density.

Colistin damages the CM by disrupting cation bridges between LPS molecules

To understand how colistin targeting of LPS in the CM leads to membrane disruption, we studied the role of cation bridges which are crucial for stabilising interactions between LPS molecules, by exposing spheroplasts from *E. coli* pEmpty cells to colistin in the absence or presence of excess magnesium. In keeping with a role for cation bridges, we found that magnesium chloride conferred dose-dependent protection from colistin-mediated CM disruption (Fig. 3A). To rule out a general protective osmotic effect from the higher salt concentration, we demonstrated that identical concentrations of sodium chloride did not protect

220 spheroplasts from colistin (Fig. 3B). Furthermore, the presence of exogenous magnesium had no significant
221 effect on reducing spheroplast CM damage caused by daptomycin or nisin (Fig. 3CD), confirming that these
222 CAMPs do not have the same CM target as colistin.

223 In conclusion, our findings demonstrate that colistin targets LPS in the CM of polymyxin-susceptible *E. coli*,
224 leading to the displacement of cationic inter-LPS bridges, membrane disruption and ultimately bacterial lysis.
225 This is similar to the mechanism by which colistin disrupts the OM of bacteria and synthetic phospholipid
226 bilayer membranes containing low levels of LPS [17,44-45]. However, the high levels of LPS modified by pEtN
227 in the CM of MCR-1-producing *E. coli* prevent colistin from targeting LPS in the CM, protecting the membrane
228 and conferring resistance to the polymyxin antibiotic.

229

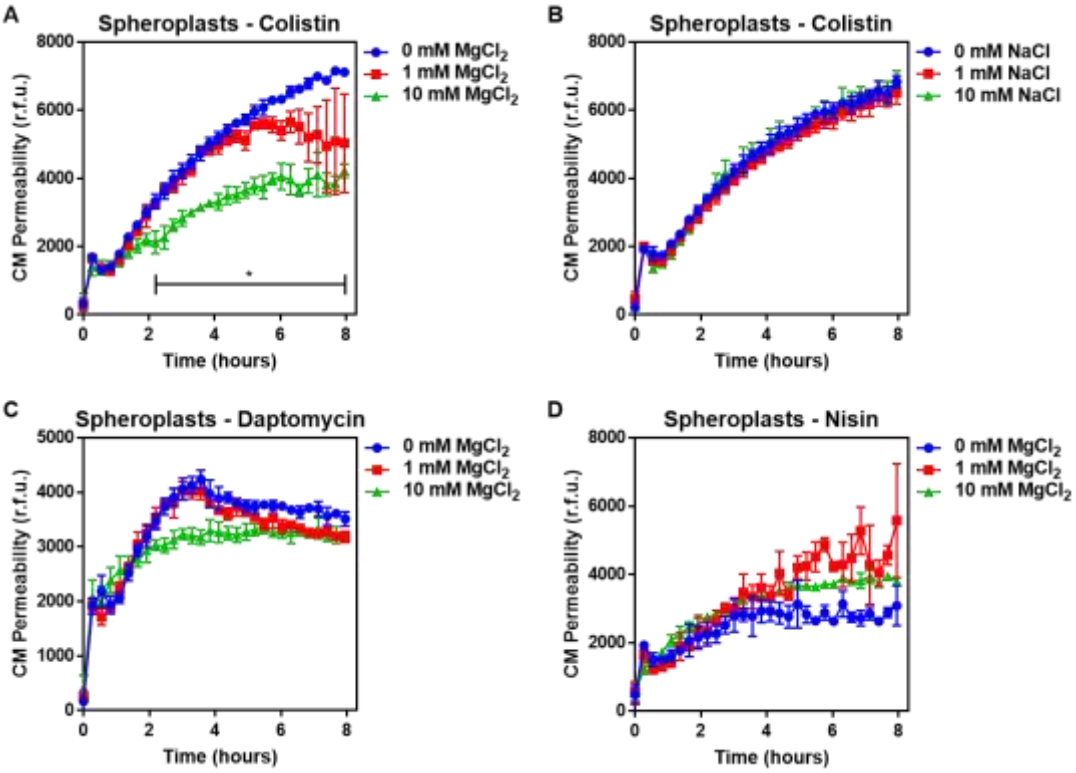

230

231 **Figure 3. Colistin damages the cytoplasmic membrane by disrupting cation bridges between LPS molecules. A, B,**
232 Permeabilization of the CM of *E. coli* MC1000 spheroplasts generated from empty plasmid control bacteria during
233 incubation with colistin (4 µg ml^{-1}), in the absence or presence of either $MgCl_2$ **(A)** or NaCl **(B)** at the indicated
234 concentrations, as determined using 0.25 µM PI (n=3, experiment performed on 3 independent occasions; *p<0.01
235 between 0 mM $MgCl_2$ and 10 mM $MgCl_2$). **C, D,** Permeabilization of the CM of *E. coli* MC1000 spheroplasts generated
236 from empty plasmid control bacteria during incubation with either **(C)** daptomycin (20 µg ml^{-1}, with 1.25 µM Ca^{2+} ions)
237 or **(D)** nisin (20 µg ml^{-1}), in the absence or presence of $MgCl_2$ at the indicated concentrations, as determined using 0.25
238 µM PI (n=3, experiment performed on 3 independent occasions). Data in **A-D** were analysed by a two-way ANOVA with
239 Dunnett's post-hoc test. Data are presented as the arithmetic mean, and error bars represent the standard deviation of
240 the mean. CM: cytoplasmic membrane; r.f.u.: relative fluorescence units.

241 **Murepavadin-triggered LPS accumulation in the cytoplasmic membrane sensitises *P. aeruginosa* to colistin**

242 Having determined that colistin kills bacteria by targeting LPS in the CM, we wanted to use this information
243 to develop a new therapeutic approach to enhance colistin efficacy.

244 Murepavadin is a first in class peptide-based inhibitor of the LptD component of the LptABCDEFG complex of
245 *P. aeruginosa* that transports LPS from the CM to the OM [46]. Thus, inhibition of the Lpt system in *P.*
246 *aeruginosa* leads to LPS accumulation in the CM, which we hypothesised would increase the susceptibility of
247 the bacterium to colistin [46,47].

248 To test our hypothesis, we first used a checkerboard MIC assay and found that colistin synergised with
249 murepavadin against *P. aeruginosa* PA14 cells, revealing that sub-lethal concentrations of the LptD inhibitor
250 sensitised the bacterium to colistin (Fig. 4A) [48]. To confirm that sub-lethal concentrations of murepavadin
251 altered LPS abundance in the CM, *P. aeruginosa* was incubated with murepavadin, before the amount of LPS
252 in whole cells and spheroplasts was measured using the well-established Limulus Amoebocyte Lysate (LAL)
253 assay (Supplementary Fig. 6, 7) since previous work has shown this approach to be a highly accurate way of
254 quantifying LPS in whole cell lysates [49]. The suitability of the LAL assay was further confirmed using a
255 MALDI-TOF-based lipidomic analysis of spheroplast lysates, which confirmed that the LPS in both
256 murepavadin-exposed and untreated bacteria was unmodified and thus able to be accurately detected and
257 quantified (Supplementary Fig. 8) [50]. Sub-lethal concentrations of murepavadin caused a slight reduction
258 in LPS levels in the OM of *P. aeruginosa* cells, but a significant increase in the amount of LPS in the CM
259 compared to untreated spheroplasts (Supplementary Fig. 8, 9). Moreover, our lipidomic analysis revealed
260 that the ratio of lipid A:phospholipid increased in *P. aeruginosa* spheroplasts pre-exposed to murepavadin,
261 confirming that the LptD inhibitor caused LPS to accumulate in the CM (Supplementary Fig. 8).

262 Next, we proceeded to test whether LPS accumulation in the CM increased the susceptibility of *P. aeruginosa*
263 to colistin. We started by examining the effect of colistin on the OM and CM of *P. aeruginosa* exposed, or
264 not, to murepavadin. Despite the slight reduction of LPS at the OM caused by murepavadin, colistin
265 permeabilized the OM to the same extent as bacteria that had not been exposed to murepavadin, with similar
266 levels of NPN uptake (Fig. 4B). By contrast, however, murepavadin significantly enhanced permeabilization
267 of the CM by colistin in whole cells of *P. aeruginosa*, as determined via uptake of PI (Fig. 4C). Thus, an increase
268 in LPS levels in the CM promoted colistin-mediated damage, in keeping with our conclusion that LPS in the
269 CM is the target of the polymyxin antibiotic. Furthermore, *P. aeruginosa* cells exposed to murepavadin were
270 more rapidly lysed by colistin than untreated cells, confirming that LPS accumulation in the CM increased
271 susceptibility to the polymyxin antibiotic (Fig. 4D).

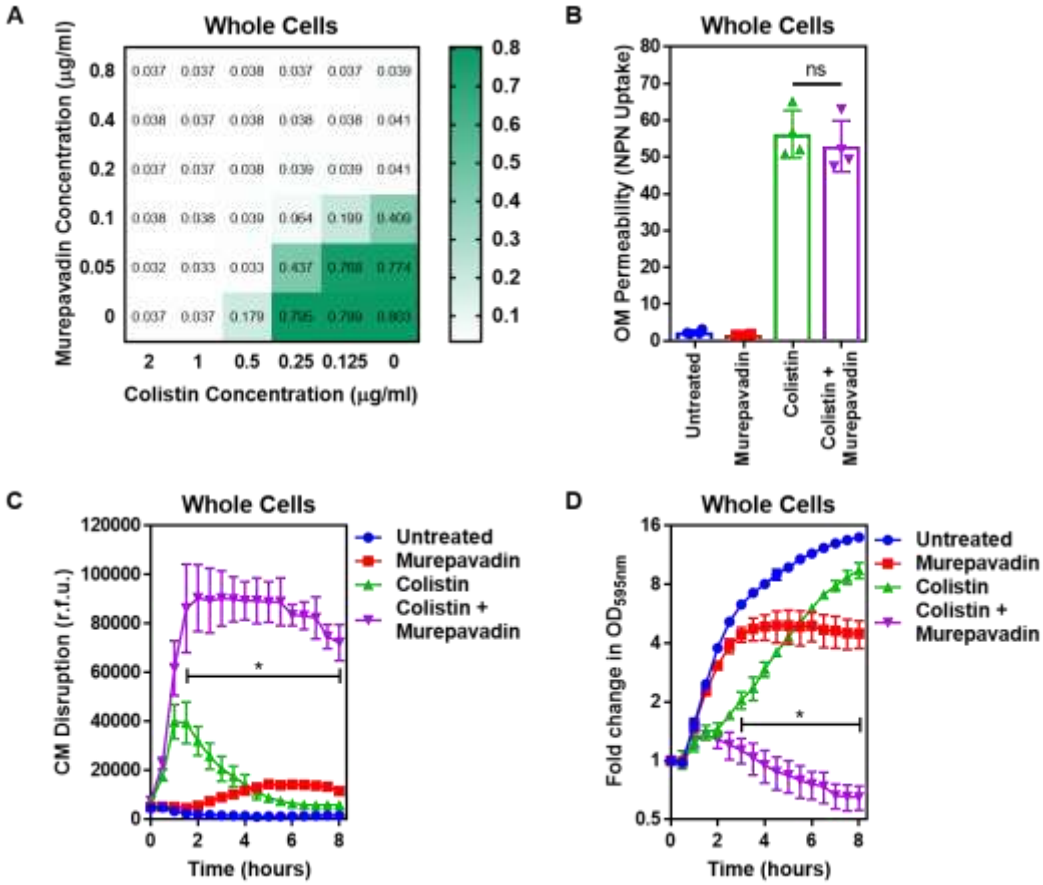

Figure 4. Murepavadin sensitises *P. aeruginosa* to colistin by increasing LPS abundance in the cytoplasmic membrane. **A,** Checkerboard broth microdilution assay showing the synergistic growth-inhibitory interaction between colistin and the LPS transport inhibitor murepavadin against *P. aeruginosa* PA14 cells, as determined by measuring OD_{595nm} after 18 hours incubation. **B,** OM disruption of *P. aeruginosa* PA14 cells during 10 minutes exposure to colistin (2 µg ml^{-1}) in the absence or presence of murepavadin (0.05 µg ml^{-1}), as assessed by uptake of the fluorescent dye NPN (10 µM) (n=4, each data point represents the arithmetic mean of 20 replicate measurements; ns: p>0.05 between colistin-treated bacteria). **C,** CM disruption of *P. aeruginosa* PA14 cells exposed to colistin (2 µg ml^{-1}) in the absence of presence of murepavadin (0.05 µg ml^{-1}), as determined using 2.5 µM PI (n=4; *p<0.0001 for Colistin and Murepavadin-exposed cells compared to Colistin alone). **D,** Lysis of *P. aeruginosa* PA14 cells exposed to colistin (2 µg ml^{-1}) in the absence of presence of murepavadin (0.05 µg ml^{-1}), as measured by OD_{595nm} readings (n=4; *p<0.01 for Colistin and Murepavadin-exposed cells compared to Colistin alone). Data in **B** were analysed by a one-way ANOVA with Tukey's post-hoc test. Data in **C-D** were analysed by a two-way ANOVA with Dunnett's post-hoc test. Data are presented as the arithmetic mean, and error bars represent the standard deviation of the mean. OM: outer membrane; NPN: *N*-phenyl-1-naphthylamine; CM: cytoplasmic membrane; r.f.u.: relative fluorescence units; OD: optical density.

288 **Combination therapy with colistin and murepavadin promotes clearance of *P. aeruginosa***

289 Having shown that murepavadin sensitised the CM to colistin-mediated damage, we wanted to determine
290 whether this translated into enhanced antibacterial activity against relevant clinical isolates and increased
291 treatment efficacy *in vivo*. We found that a sub-lethal concentration of murepavadin sensitised *P. aeruginosa*
292 PA14 to a normally sub-lethal concentration of colistin (2 µg ml^{-1}), resulting in >10,000-fold reduction in c.f.u.
293 counts relative to bacteria incubated with murepavadin or colistin alone after 8 h (Fig. 5A). We also found
294 that murepavadin potentiated the activity of an even lower concentrations of colistin (1 µg ml^{-1}), with
295 exposure to the LPS transport inhibitor increasing the ability of the polymyxin antibiotic to damage the CM,
296 triggering bacterial lysis and cell death (Supplementary Fig. 10).

297 We next examined a panel of 16 multi-drug resistant *P. aeruginosa* clinical strains, isolated from the sputum
298 of cystic fibrosis (CF) patients, to investigate whether murepavadin increased colistin-mediated bacterial
299 killing (Supplementary Fig. 11). Of these 16 clinical isolates, 14 were susceptible to murepavadin alone, whilst
300 two strains were resistant to the LptD inhibitor (Supplementary Table 2). In 11 out of 14 murepavadin-
301 susceptible CF isolates tested (79%), sub-lethal concentrations of murepavadin caused a significant increase
302 in the bactericidal activity of colistin against *P. aeruginosa* (Fig. 5B). Importantly, murepavadin did not affect
303 the bactericidal activity of colistin against the two strains that were resistant to LptD inhibitor (Fig. 5B). This
304 confirmed that the potentiating effects of the LptD inhibitor on polymyxin-mediated killing were not due to
305 off-target effects.

306 Next, we wanted to test whether colistin-murepavadin dual therapy could promote bacterial clearance
307 during infection *in vivo*. We inoculated mice via the intranasal route with *P. aeruginosa* PA14 to cause a lung
308 infection, and then treated intranasally with PBS alone, or PBS containing colistin only (5 mg kg^{-1}),
309 murepavadin only (0.25 mg kg^{-1}), or colistin and murepavadin combined at the concentrations used for mono-
310 treatment. These concentrations were based on those used previously to mimic treatment of human lung
311 infections, and the route of delivery is similar to that used clinically [51-54]. Mono-therapy with colistin alone
312 or murepavadin alone had very little effect on the bacterial load assessed after 3 hours treatment compared
313 with the no-treatment control (Fig. 5C). By contrast, combination therapy with colistin and murepavadin
314 caused a ~500-fold reduction in c.f.u. counts relative to the no-treatment control (Fig. 5C). Therefore,
315 murepavadin synergises with colistin both *in vitro* and *in vivo*, suggesting it may be useful as a combination
316 therapeutic approach for lung infections caused by *P. aeruginosa*.

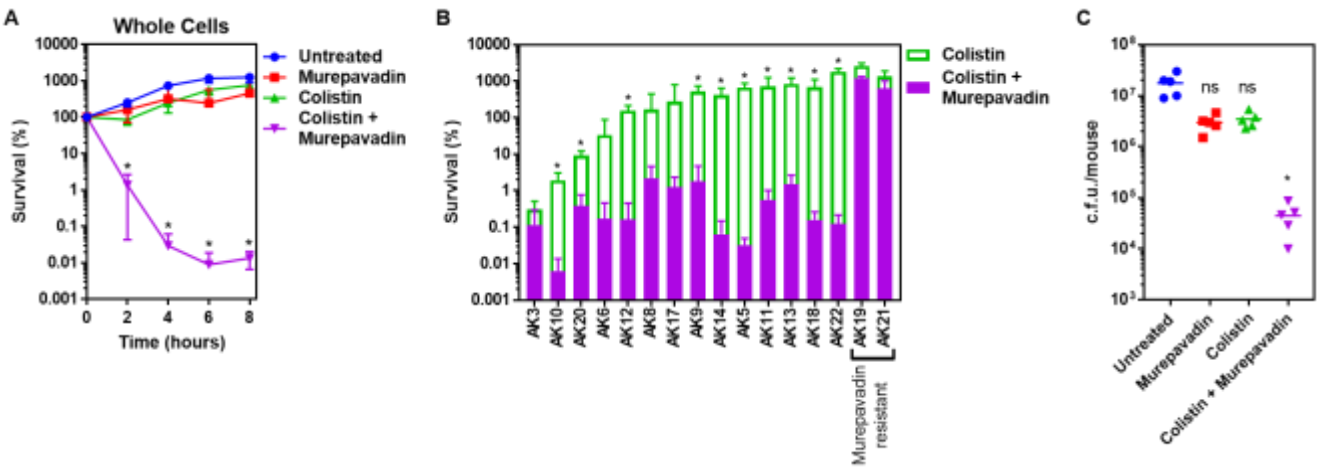

317

318 **Figure 5. Colistin-murepavadin combination therapy promotes killing of *P. aeruginosa in vitro* and *in vivo*. A,** Survival
319 of *P. aeruginosa* PA14 cells exposed to colistin (2 µg ml^{-1}) in the absence of presence of murepavadin (0.05 µg ml^{-1}), as
320 determined by c.f.u. counts (n=4; *p<0.05 for Colistin and Murepavadin-exposed cells compared to Colistin alone). **B,**
321 Survival or growth of a panel of clinical multidrug-resistant *P. aeruginosa* strains isolated from the sputum of cystic
322 fibrosis patients after 8 hours exposure to colistin (2 µg ml^{-1}) alone, or in the presence of a sub-lethal concentration
323 (0.5x MIC) of murepavadin, as determined by c.f.u. counts (n=4; *p<0.01 for Colistin and Murepavadin-exposed cells
324 compared to Colistin alone). **C,** Burden of *P. aeruginosa* PA14 in the lungs of mice after 3 hours treatment with
325 murepavadin (0.25 mg/kg), colistin (5 mg/kg), neither antibiotic, or both antibiotics in combination, as determined by
326 c.f.u. counts (each data point represents a single mouse; for each group, n=5; ns: p>0.05, *p<0.001 compared to
327 Untreated mice). Data in **A-B** were analysed by a two-way ANOVA with Dunnett's **(A)** or Sidak's **(B)** post-hoc tests. Data
328 in **C** were analysed by a Kruskal-Wallis test with Dunn's post-hoc test. Data are presented as the arithmetic mean, and
329 error bars, where shown, represent the standard deviation of the mean.

330

331 **Discussion**

332 Colistin is an increasingly important last-resort antibiotic used to treat infections caused by multi-drug-
333 resistant Gram-negative pathogens, including *P. aeruginosa*, *K. pneumoniae* and *E. coli* [2-4]. However,
334 treatment failure occurs frequently, and resistance is a growing concern [5-10]. Efforts to address these
335 issues are compromised by a poor understanding of colistin's bactericidal mode of action. Whilst the initial
336 interactions of colistin with LPS in the OM of Gram-negative bacteria were well-established, it was unclear
337 how the antibiotic traversed the OM and damaged the CM to cause cell lysis (Supplementary Fig. 1). In this
338 work, we demonstrate that colistin targets LPS in the CM, resulting in membrane permeabilization, bacterial
339 lysis and killing (Fig. 6).

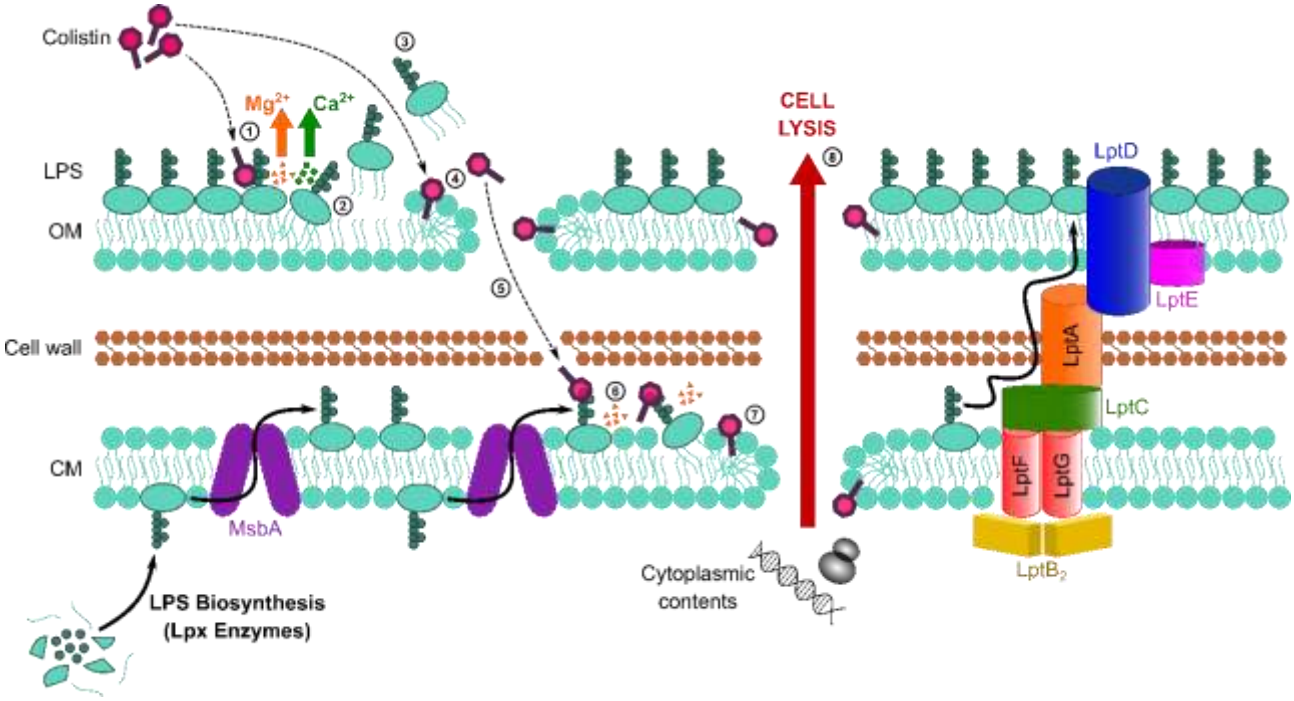

340

341 **Figure 6. Colistin kills bacteria by targeting LPS in both the outer and cytoplasmic membranes, leading to disruption**
342 **of the cell envelope and bacterial lysis.** Diagrammatic representation of the novel proposed mechanism of action of
343 colistin: Colistin binds to LPS in the OM (1), displacing cations that form bridges between LPS molecules, which leads to
344 destabilisation of the OM (2). As a consequence of the weakening of intermolecular bonds in the LPS monolayer, LPS is
345 released from the bacterial surface (3), allowing colistin to further damage the OM via the action of the polymyxin lipid
346 tail (4). This provides colistin with access to the periplasm, where colistin interacts with LPS in the CM (5) that is awaiting
347 transport to the OM by the LptABCDEFG machinery after being synthesized in the cytoplasm and flipped to the outer
348 leaflet of the CM by MsbA. As in the OM, colistin binding to LPS results in displacement of cation bridges and disruption
349 of the CM (6), which it ultimately permeabilizes (7), culminating in the loss of cytoplasmic contents, cell lysis and
350 bacterial death (8).

351

352 Our conclusion that colistin targets LPS in the CM was based initially on experiments with *E. coli* expressing
353 the *mcr*-1 colistin resistance determinant. MCR-1 modifies lipid A with a phosphoethanolamine moiety as it
354 passes through the CM on its way to the OM [21,23]. Since MCR-1 specifically protected spheroplasts from
355 colistin but not nisin or daptomycin, which both target phospholipid bilayers, it was clear that colistin did not
356 share the same target as the other two CAMPs. Given the only difference between *E. coli* spheroplasts
357 expressing *mcr*-1 and pEmpty spheroplasts was modified LPS, our data reveal that colistin targets LPS in the
358 CM, leading to disruption of the CM, which is a pre-requisite for subsequent cell lysis and bacterial killing
359 [38]. These findings were then supported by experiments showing that LPS accumulation in the CM of *P.*
360 *aeruginosa* sensitised this bacterium to colistin.

361 Whilst the abundance of LPS in the CM is 10-20 times lower than the OM, studies with model membranes
362 have shown that the presence of LPS at a 1:100 ratio with phospholipids was both necessary and sufficient
363 for colistin-mediated permeabilization [17,42-43]. Therefore, our conclusion explains how an antibiotic with
364 a high degree of specificity for LPS could damage both the OM and CM [1]. The reason why MCR-1 protected
365 the CM but not OM from colistin-mediated damage is most likely due to the higher proportion of unmodified
366 LPS at the CM (21±2%) relative to the OM (42±19%) (Fig. 1A). Furthermore, the overall abundance of LPS in
367 the CM is very low, resulting in very few targets (i.e. unmodified LPS molecules) for colistin in the CM of *mcr-*
368 *1*-expressing *E. coli*. By contrast, the OM of MCR-1-producing *E. coli* contains many more unmodified LPS
369 molecules that can be bound by colistin, explaining why colistin is able to damage this structure, but cannot
370 permeabilize the CM of *E. coli* expressing *mcr-1* at a physiologically relevant concentration [42,43]. Whether
371 colistin resistance conferred by chromosomal mutations in two-component systems is also mediated by
372 modified LPS in the CM remains to be tested [22-27].

373 Our data showing that colistin requires unmodified LPS to be present in the CM in order to kill bacteria
374 explains how an antibiotic with high affinity and specificity for LPS causes disruption to both the OM and CM
375 [1]. Furthermore, these findings provide support for the observations that colistin does not damage the OM
376 of colistin-resistant *A. baumannii* isolates where LPS has been replaced by a phospholipid bilayer, and that
377 polymyxins cause only minimal disruption to model phospholipid membranes unless LPS is present [17-20].

378 Whilst the interaction of colistin with LPS in the CM is likely to share similarities with the same process at the
379 OM, there are also likely to be differences owing to the differing concentrations of LPS between the two
380 membranes [17,42-43]. In the OM, LPS is a highly abundant component with molecules tightly packed and
381 stabilised with cation bridges. By contrast, LPS is a minority component in the CM, which may affect the rate
382 and degree to which the CM is disrupted by polymyxins. In support of this, whilst colistin induced OM damage
383 within minutes of bacterial exposure to the antibiotic, disruption of the CM took much longer. Even when
384 spheroplasts lacking an OM were exposed to colistin, it still took more than 2 hours for CM permeabilization
385 to occur. Therefore, it appears that colistin-mediated disruption of the CM is considerably less efficient than
386 that of the OM, likely due to the much lower levels of LPS present in the CM.

387 Combined, these findings provide strong evidence that colistin targets LPS in the CM, in addition to the OM,
388 and that this is required for the bactericidal and lytic activity of the antibiotic at clinically relevant
389 concentrations. This insight into the mode of action of colistin enabled us to devise a new therapeutic
390 approach to enhance colistin efficacy. Using the LptD inhibitor murepavadin, which is in development as an
391 inhaled treatment for *P. aeruginosa* infections, we triggered LPS accumulation in the CM, and thereby
392 increased the susceptibility of bacteria to colistin. The potential clinical utility of this approach was
393 demonstrated by showing enhanced activity of colistin-murepavadin combination therapy against a panel of
394 clinical CF isolates, as well as potent efficacy in a murine model of *P. aeruginosa* lung infection. It is
395 anticipated that a combination of colistin and murepavadin could enhance the low treatment efficacy of
396 polymyxin antibiotics and may also limit the toxic side effects associated with both compounds by enabling
397 the use of lower doses of the drugs [55].

398 In summary, this work contributes to our understanding of the mechanism of action of colistin by
399 demonstrating that polymyxin antibiotics target LPS in both the OM and the CM, and that this leads to the
400 disruption of both membranes, resulting in the bactericidal and lytic activities of the antibiotic. Modulation
401 of LPS levels can enhance colistin activity, providing the foundations for new approaches to enhance the
402 efficacy of this antibiotic of last resort.

403

404 ## Methods

405 **Bacterial strains and growth conditions**

406 The bacterial strains used in this study are listed in Supplementary Table 1. For each experiment, all strains
407 were grown in Luria broth (LB; Thermo Fisher Scientific, USA) for 18 h to stationary phase at 37°C with shaking
408 (180 r.p.m.). For routine culture of bacteria on solid media, strains were grown on LB supplemented with
409 1.5% technical agar (BD Biosciences, USA). Liquid and solid growth media were supplemented with
410 tetracycline (12.5 µg ml^{-1}; Sigma-Aldrich, USA) and 0.5 mM isopropyl-β-D-thiogalactoside (IPTG, Melford
411 Laboratories, UK) where required. Enumeration of bacterial c.f.u. was done by plating 10-fold serial dilutions
412 of bacterial cultures on to Mueller-Hinton agar (MHA; Thermo Fisher Scientific) plates. Inoculated agar plates
413 were incubated statically for 18 h in air at 37°C.

414 **Determination of minimum inhibitory concentrations of antibiotics**

415 The minimum inhibitory concentration (MIC) of colistin and murepavadin against bacterial strains was
416 determined by the broth microdilution protocol [56]. A microtitre plate was used to prepare a range of
417 antibiotic concentrations in 200 µl cation-adjusted Mueller-Hinton broth (CA-MHB; Thermo Fisher Scientific)
418 by two-fold serial dilutions. For certain experiments, checkerboard analyses were performed by preparing
419 two-fold serial dilutions of two antibiotics in different directions, generating an 8 x 8 matrix to assess the
420 MICs of the antibiotics in combination [48]. Stationary-phase bacteria were diluted 1000-fold in fresh CA-
421 MHB and seeded into each well of the microtitre plate to a final concentration of 5 x 10^5 c.f.u. ml^{-1}. The
422 microtitre plates were then incubated statically at 37°C for 18 h in air, after which point the MIC was defined
423 as the lowest antibiotic concentration at which there was no visible growth of bacteria. In some cases, the
424 extent of bacterial growth after 18 h incubation was also determined by obtaining OD_{595nm} measurements
425 using a Bio-Rad iMark microplate absorbance reader (Bio-Rad Laboratories, USA).

426 **Bacterial growth assay**

427 Stationary-phase bacteria were diluted 1000-fold in fresh CA-MHB, and 4 µl was seeded into the wells of a
428 microtitre plate containing 200 µl CA-MHB, and for some experiments the LptD inhibitor murepavadin, to
429 give a final inoculum of 5 x 10^5 c.f.u. ml^{-1}. The microtitre plate was incubated with shaking (180 r.p.m.) at
430 37°C for 16 h in a Tecan Infinite 200 Pro multiwell plate reader (Tecan Group Ltd., Switzerland) and optical
431 density measurements were taken at 600 nm every 15 min.

432 **Production of spheroplasts**

433 Spheroplasts of *E. coli* and *P. aeruginosa* strains lacking an OM and cell wall were generated as previously
434 described [35]. Briefly, stationary-phase bacteria grown overnight were washed twice by centrifugation
435 (12,300 x *g*, 3 min) followed by resuspension in CA-MHB, and added at a final inoculum of 10^8 c.f.u. ml^{-1} to 9

436 ml CA-MHB containing for some experiments the LPS transport inhibitor murepavadin. Cultures were then
437 incubated at 37°C with shaking (180 r.p.m.) for 2 h. After the incubation, bacteria were washed twice by
438 centrifuging (3,273 x *g*, 20 min, 4°C) and resuspending first in 10 ml Tris buffer (0.03 M, pH 8.0; Sigma-Aldrich),
439 and subsequently in Tris buffer (0.03 M, pH 8.0) containing 20% sucrose. EDTA (250 µl, 10 mg ml^{-1}; Sigma-
440 Aldrich) and lysozyme (1 ml, 10 mg ml^{-1}; Roche, Switzerland) were added to remove the OM and cell wall
441 respectively, and the cell suspension was incubated for 1 h in a water bath shaker at 30°C. Trypsin (500 µl,
442 10 mg ml^{-1}; Sigma-Aldrich) was then added, and the culture again incubated at 30°C in a water bath shaker
443 for 15 min. The resulting spheroplasts produced were harvested by mild centrifugation (2,000 x *g*, 20 min,
444 4°C), with the supernatant containing the removed OM extracted for further analysis. Successful conversion
445 of bacterial whole cells into spheroplasts was confirmed using phase-contrast microscopy, as detailed below.

446 **Confirmation of successful spheroplast formation**

447 Whole cells of *E. coli* and *P. aeruginosa* grown overnight were washed twice by centrifugation (12,300 x *g*, 3
448 min) and resuspension in CA-MHB, added at a final inoculum of 10^8 c.f.u. ml^{-1} to 9 ml CA-MHB, and incubated
449 for 2 h at 37°C with shaking (180 r.p.m.). Outer membrane proteins of these bacteria were subsequently
450 labelled with fluorescein isothiocyanate (FITC, Sigma-Aldrich) as previously described [57]. Bacterial cells
451 were washed twice by centrifugation (3,273 x *g*, 20 min, 4°C) and resuspension in 10 ml Labelling Buffer
452 (50mM Na_2CO_3, 100 mM NaCl, pH 8.0), to which FITC was added at a final concentration of 0.5 mg ml^{-1}.
453 Bacteria were incubated for 30 mins at room temperature, before labelled cells were harvested by
454 centrifuging (3,273 x *g*, 20 min, 4°C) and washed thrice by resuspending in 10 ml Tris buffer (0.03 M, pH 8.0)
455 containing 20% sucrose. 1 ml of FITC-labelled bacteria was extracted and centrifuged (12,300 x *g*, 3 min), and
456 the cells were fixed in 4% paraformaldehyde (PFA) in phosphate-buffered saline (PBS). The remaining 9 ml of
457 FITC-labelled cells were converted into spheroplasts, as described above. The spheroplasts produced were
458 recovered by mild centrifugation (2,000 x *g*, 20 min, 4°C) and resuspension in 9 ml Tris buffer (0.03 M, pH
459 8.0) containing 20% sucrose, before 1 ml of spheroplasts were fixed in the same way as with whole cells. The
460 amount of FITC fluorescence in the OM of whole cells and CM of spheroplasts was observed using
461 fluorescence microscopy, as described below. For quantification of FITC fluorescence, 200 µl samples of the
462 fixed bacterial suspensions were seeded into the wells of a black-walled microtitre plate, and fluorescence
463 measured with a Tecan Infinite 200 Pro multiwell plate reader, using an excitation wavelength of 490 nm and
464 an emission wavelength of 525 nm.

465 **Microscopy**

466 For phase-contrast and fluorescence microscopy, a 5 µl sample of fixed bacterial whole cells or spheroplasts
467 was spotted onto a thin 1.2% agarose gel patch prepared in distilled water on a microscope slide. Bacteria
468 were imaged using an Axio Imager.A2 Zeiss microscope (Carl Zeiss Microscopy GmbH, Germany) at 1000x
469 magnification with an oil immersion objective lens. The ZEN 2012 software was used for image acquisition,

470 whilst analysis of cell length:width ratios was done using the FIJI/ImageJ software by measuring two
471 perpendicular lines drawn through the centre of bacteria. For each experiment, all microscopy images were
472 acquired and processed using identical settings throughout.

473 **Determination of LPS concentration and modification by mass spectroscopy**

474 Spheroplasts from bacterial cells were prepared as described above and then resuspended in ddH_2O (200 µl),
475 before mild acid hydrolysis was performed via the addition of 2% (vol/vol) acetic acid in ddH_2O (200 µl) and
476 incubation at 100°C for 30 min. For experiments with whole cells, bacteria grown overnight to stationary-
477 phase were washed three times by centrifuging and resuspending in ddH_2O, and a mild acid hydrolysis was
478 performed on these whole cells as described for spheroplasts. Acid-treated whole cells or spheroplasts were
479 recovered by centrifugation (17,000 × *g*, 2 min), and the resulting pellet was washed before being
480 resuspended in 50 µl ultrapure water. The whole cell or spheroplast suspension (0.5 µl) was then loaded
481 immediately onto the target and overlaid with 1.2 µl of a matrix consisting of 9H-Pyrido[3,4-B]indole
482 (Norharmane) (Sigma-Aldrich) dissolved in 90:10 (vol/vol) chloroform/methanol to a final concentration of
483 10 mg ml^{-1}. The bacterial suspension and matrix were then mixed on the target before gentle drying under
484 air at room temperature. MALDI-TOF mass spectroscopy analysis was undertaken with a MALDI Biotyper
485 Sirius system (Bruker Daltonics, USA), using the linear negative-ion mode as described previously [36].
486 Manual peak picking at masses relevant to phospholipids or lipid A was performed on the mass spectra
487 obtained, and the corresponding signal intensities at the defined masses were determined. Peaks were
488 considered only if their signal/noise ratio was at least 5. To determine the ratio of modified lipid A to
489 unmodified lipid A, the area under the pETN-modified lipid A peak (*m/z* 1,919.2) was divided by the area
490 under the peak corresponding to native lipid A (*m/z* 1,796.2). To determine the relative abundance of LPS,
491 the sum of the area under the lipid A peaks (*m/z* 1447-1700) was divided by the sum of the area under
492 representative phospholipid peaks (phospholipid 34:1,2, *m/z* 717-747). All mass spectra were generated and
493 analysed with three biological replicates and two technical replicates.

494 **Outer membrane disruption assay**

495 To detect damage to the OM of bacteria, the well-established NPN uptake assay was used [37]. Stationary-
496 phase bacterial cells were washed in fresh CA-MHB and diluted to an optical density (OD_{600nm}) of 0.5 in 5 mM
497 pH 7.2 HEPES buffer (Sigma-Aldrich). This bacterial suspension was added to wells containing the relevant
498 antibiotics in HEPES buffer, as well as the fluorescent probe *N*-phenyl-1-naphthylamine (NPN; Acros Organics,
499 USA) at a final concentration of 10 µM. Samples were placed in a black microtitre plate with clear-bottomed
500 wells and fluorescence measured immediately in a Tecan Infinite 200 Pro multiwell plate using an excitation
501 wavelength of 355 nm and an emission wavelength of 405 nm. Fluorescence measurements were obtained
502 every 30 seconds for 10 min, and the degree of OM permeabilization, referred to as the NPN Uptake Factor,
503 was calculated using the following formula:

504 $$\frac{Fluorescence\ of\ sample\ with\ NPN - Fluorescence\ of\ sample\ without\ NPN}{Fluorescence\ of\ HEPES\ buffer\ with\ NPN - Fluorescence\ of\ HEPES\ buffer\ without\ NPN}$$

505 **Cytoplasmic membrane disruption assay**

506 To measure CM disruption of whole cells, bacteria grown to stationary-phase overnight were washed and
507 inoculated into 3 ml MHB containing the relevant antibiotics. Cultures were incubated at 37°C with shaking
508 (180 r.p.m.) for up to 8 h, and every 30 min, aliquots (200 µl) were taken and bacteria isolated by
509 centrifugation (12,300 x *g*, 3 min). Cells were then washed in sterile PBS before being added to the wells of a
510 black-walled microtitre plate, and propidium iodide (PI, Sigma-Aldrich) was added to each well at a final
511 concentration of 2.5 µM. Fluorescence was measured immediately in a Tecan Infinite 200 Pro multiwell plate
512 reader (excitation at 535 nm, emission at 617 nm). To measure disruption of the CM in spheroplasts,
513 spheroplasts of *E. coli* generated as detailed above were washed by centrifugation (4,000 x *g*, 5 min) and
514 resuspension in Tris buffer (0.03 M, pH 8.0) containing 20% sucrose. Spheroplast samples (20 µl) were then
515 added in the wells of a black-walled microtitre plate to 180 µl of Tris buffer (0.03 M, pH 8.0) containing 20%
516 sucrose, the relevant antibiotics, and PI at a final concentration of 0.25 µM. The microtitre plate was
517 incubated with shaking (180 r.p.m.) at 37°C for up to 8 h in a Tecan Infinite 200 Pro multiwell plate reader
518 and fluorescence (excitation at 535 nm, emission at 617 nm) measured every 15 min. For both whole bacterial
519 cells and spheroplasts, to account for differences in fluorescence values arising from variations in cell
520 number, relative fluorescence unit (r.f.u.) measurements were corrected for OD at 600 nm.

521 **Determination of bacterial lysis**

522 In the case of whole bacterial cells, washed stationary-phase bacteria were inoculated into 3 ml CA-MHB
523 containing the relevant antibiotics, as described above. Cultures were then placed in a shaking incubator
524 (37°C, 180 r.p.m.) for 8 h, and every 30 min, samples (200 µl) were transferred to a microtitre plate, where
525 OD_{595nm} measurements were obtained using a Bio-Rad iMark microplate absorbance reader. For
526 spheroplasts, washed spheroplasts (20 µl) were added to 180 µl of Tris buffer (0.03 M, pH 8.0) containing
527 20% sucrose and the relevant antibiotics in a microtitre plate as detailed above. The microtitre plate was
528 incubated for up to 8 h at 37°C with shaking (180 r.p.m.) in a Tecan Infinite 200 Pro multiwell plate reader,
529 and readings of OD_{600nm} were made every 15 min.

530 **Determination of LPS concentration by Limulus Amebocyte Lysate assay**

531 Stationary-phase bacteria grown overnight were washed and grown for 2 h, before conversion to
532 spheroplasts as described above. During formation of spheroplasts, the OM extracted from the bacterial cells
533 was recovered, and the concentration of LPS in the OM, as well as the concentration of LPS in the CM of
534 spheroplasts, was determined using the chromogenic Limulus Amebocyte Lysate (LAL) assay (all reagents
535 from Thermo Fisher Scientific) as described previously [49-50, 58]. OM samples and spheroplasts lysed by
536 freeze-thaw to release LPS were diluted in 10-fold steps, and 50 µl of each sample was equilibrated to 37°C

537 and loaded into the wells of a microtitre plate at the same temperature. LAL reagent (50 µl) was added to
538 each well, and the mixture incubated at 37°C for 10 min. Chromogenic substrate solution (100 µl, 2 mM) was
539 subsequently added to each well and the microtitre plate was incubated for a further 6 min at 37°C. The
540 enzymatic reaction was stopped by adding 50 µl of 25% acetic acid to each well, and the presence of LPS was
541 determined by measuring absorbance at 405 nm in a Tecan Infinite 200 Pro multiwell plate reader. A standard
542 curve was generated using an *E. coli* endotoxin standard stock solution, which enabled the conversion of
543 A_{405nm} values into concentrations of LPS.

544 **Determination of bactericidal activity of antibiotics**

545 As described above, stationary-phase bacteria grown overnight were washed twice and added at a final
546 inoculum of 10^8 c.f.u. ml^{-1} to 3 ml CA-MHB containing colistin and/or murepavadin. Cultures were incubated
547 with shaking (37°C, 180 r.p.m.) for up to 8 h. Bacterial survival was determined after 2, 4, 6, and 8 h by serially
548 diluting cultures in 10-fold steps in 200 µl sterile PBS (VWR International, USA), before enumeration of c.f.u.
549 counts on MHA plates.

550 **Murine lung infection model**

551 The use of mice was performed under the authority of the UK Home Office outlined in the Animals (Scientific
552 Procedures) Act 1986 after ethical review by Imperial College London Animal Welfare and Ethical Review
553 Body (PPL 70/7969). Wild-type C57BL/6 mice were purchased from Charles River (UK). All mice were female
554 and aged between six to eight weeks. Mice were housed with five per cage with Aspen chip 2 bedding and
555 12 h light/dark cycles at 20–22 °C. Mice were randomly assigned to experimental groups. Water was provided
556 *ad libitum* and mice were fed RM1 (Special Diet Services). To establish colonisation of the lungs, mice were
557 anesthetized and intranasally inoculated with 10^7 c.f.u. of *P. aeruginosa* PA14 in 50 µL of PBS, as described
558 previously [59,60]. Infection was allowed to establish for 5 h, before mice were again anaesthetized and
559 treated via the intranasal route with 50 µL of PBS alone, or PBS containing colistin (5 mg kg^{-1}), murepavadin
560 (0.25 mg kg^{-1}), or a combination of colistin and murepavadin for 3 h. To enumerate bacterial load in the lungs,
561 mice were humanely sacrificed, their lungs removed and homogenized in PBS, and then plated onto
562 *Pseudomonas* isolation agar (Thermo Fisher Scientific).

563 **Statistical analyses**

564 Experiments were performed on at least three independent occasions, and the resulting data are presented
565 as the arithmetic mean of these biological repeats, unless stated otherwise. Error bars, where shown,
566 represent the standard deviation of the mean. For single comparisons, a two-tailed Student's *t*-test was used
567 to analyse the data. For multiple comparisons at a single time point or concentration, data were analysed
568 using a one-way analysis of variance (ANOVA) or a Kruskal-Wallis test. Where data were obtained at several
569 different time points or concentrations, a two-way ANOVA was used for statistical analyses. Appropriate
570 post-hoc tests (Dunnett's, Tukey's, Sidak's, Dunn's) were carried out to correct for multiple comparisons,

571 with details provided in the figure legends. Asterisks on graphs indicate significant differences between data,
572 and the corresponding p-values are reported in the figure legend. All statistical analyses were performed
573 using GraphPad Prism 7 software (GraphPad Software Inc., USA).

574

575 **Acknowledgements**

576 Aishwarya Krishna, Laura Nolan, Alain Filloux, Ollie Fletcher (all Imperial College London) and Alireza
577 Abdolrasouli (Imperial College Healthcare NHS Trust) are gratefully acknowledged for providing bacterial
578 strains. Lisa Haigh (Imperial College London) is thanked for processing and analysing mass spectrometry
579 samples. Vladimir Pelicic (Imperial College London) is thanked for providing access to the Axio Imager.A2
580 Zeiss microscope. A.S. is supported by a PhD studentship funded by a Medical Research Council Doctoral
581 Training Award to Imperial College London (MR/N014103/1). A.K. is funded by the DFG German Research
582 Foundation (KL3191/1-1) and the European Union's Horizon 2020 research and innovation programme under
583 the Marie Skłodowska-Curie Actions grant agreement "BacDrug" (838183). M.B. and M.M.S gratefully
584 acknowledge support from the Rosetrees Trust (M300-CD1). D.A.I.M. and R.C.D.F. gratefully acknowledge
585 funding from an MRC Career Development Award (MR/M009505/1). J.C.D is supported by the NIHR through
586 a Senior Investigator award and the Imperial Biomedical Research Centre (BRC). R.M. & J.C.D. are supported
587 by Cystic Fibrosis Trust funding. G.J.L-M. is funded by the MRC Confidence in Concept Fund and a ISSF
588 Wellcome Trust Grant (105603/Z/14/Z). T.B.C. is a Sir Henry Dale Fellow jointly funded by the Wellcome
589 Trust and Royal Society (107660/Z/15Z). L.E.E. and A.M.E. acknowledge funding from the Wellcome Trust
590 (204337/Z/16/Z). A.M.E. also acknowledges support from the National Institute for Health Research (NIHR)
591 Imperial Biomedical Research Centre (BRC), and declares funding from Shionogi & Co., Ltd for an unrelated
592 project.

593

594 **Author Contributions**

595 A.S., T.B.C. and A.M.E. designed the experiments. A.S., K.L.H.H., A.K., M.B., L.E.E., R.C.D.F., G.J.L-M., D.A.I.M.
596 and T.B.C. performed experiments or generated bacterial strains or reagents. All authors analysed data and
597 contributed to writing of the manuscript.

598

599 **Competing interests**

600 The authors declare no competing interests.

601

602 **References**

603 1. Velkov, T., Thompson, P. E., Nation, R. L., Li, J. Structure--activity relationships of polymyxin antibiotics. *J.*
604 *Med. Chem.* **53,** 1898-1916 (2010).
605 2. Garg, S. K. *et al*. Resurgence of Polymyxin B for MDR/XDR Gram-Negative Infections: An Overview of Current
606 Evidence. *Crit. Care. Res. Pract*. 3635609 (2017).
607 3. Biswas, S., Brunel, J. M., Dubus, J. C., Reynaud-Gaubert, M., Rolain, J. M. Colistin: an update on the antibiotic
608 of the 21st century. *Expert Rev. Anti. Infect. Ther.* **10,** 917-934 (2012).
609 4. Thomas, R. *et al*. The use of polymyxins to treat carbapenem resistant infections in neonates and children.
610 *Expert Opin. Pharmacother*. **20,** 415-422 (2019).
611 5. Falagas, M. E. *et al.* Colistin therapy for microbiologically documented multidrug-resistant Gram-negative
612 bacterial infections: a retrospective cohort study of 258 patients. *Int. J. Antimicrob. Agents.* **35,** 194-199
613 (2010).
614 6. Paul, M. *et al*. Colistin alone versus colistin plus meropenem for treatment of severe infections caused by
615 carbapenem-resistant Gram-negative bacteria: an open-label, randomised controlled trial. *Lancet Infect.*
616 *Dis*. **18,** 391-400 (2018).
617 7. Linden, P. K. *et al.* Use of parenteral colistin for the treatment of serious infection due to antimicrobial-
618 resistant *Pseudomonas aeruginosa*. *Clin. Infect. Dis.* **37,** e154-160 (2003).
619 8. Tran, T. B. *et al.* Pharmacokinetics/pharmacodynamics of colistin and polymyxin B: are we there yet? *Int. J.*
620 *Antimicrob. Agents.* **48,** 592-597 (2016).
621 9. Satlin, M.J. *et al*. Clinical and Laboratory Standards Institute (CLSI) and European Committee on
622 Antimicrobial Susceptibility Testing (EUCAST) position statements on polymyxin B and colistin clinical
623 breakpoints. *Clin. Infect. Dis*. (2020).
624 10. MacNair, C. R. *et al.* Overcoming *mcr-1* mediated colistin resistance with colistin in combination with other
625 antibiotics. *Nat. Commun.* **9,** 458 (2018).
626 11. Powers, J. P. S., Hancock, R. E. W. The relationship between peptide structure and antibacterial activity.
627 *Peptides* **24,** 1681–1691 (2003).
628 12. Trimble, M. J., Mlynárčik, P., Kolář M., Hancock, R. E. W. Polymyxin: Alternative Mechanisms of Action and
629 Resistance. *Cold Spring Harb. Perspect. Med.* **6,** a025288 (2016).
630 13. Berg, J. R., Spilker, C. M., Lewis, S. A. Effects of polymyxin B on mammalian urinary bladder. *J. Membr. Biol.*
631 **154,** 119-130 (1996).
632 14. Betts, J. W., Sharili, A. S., La Ragione, R. M., Wareham, D. W. *In Vitro* Antibacterial Activity of Curcumin-
633 Polymyxin B Combinations against Multidrug-Resistant Bacteria Associated with Traumatic Wound
634 Infections. *J. Nat. Prod.* **79,** 1702-1706 (2016).
635 15. Si, W., Wang, L., Usongo, V., Zhao, X. Colistin Induces *S. aureus* Susceptibility to Bacitracin. *Front. Microbiol.*
636 **9,** 2805 (2018).

637 16. Kouidhi, B., Zmantar, T., Mahdouani, K., Hentati, H., Bakhrouf, A. Antibiotic resistance and adhesion
638 properties of oral *Enterococci* associated to dental caries. *BMC Microbiol.* **11,** 155 (2011).
639 17. Khadka, N. K., Aryal, C. M., Pan, J. Lipopolysaccharide-Dependent Membrane Permeation and Lipid
640 Clustering Caused by Cyclic Lipopeptide Colistin. *ACS Omega*. **3,** 17828-17834 (2018).
641 18. Moffatt, J. H. *et al*. Colistin resistance in *Acinetobacter baumannii* is mediated by complete loss of
642 lipopolysaccharide production. *Antimicrob. Agents Chemother*. **54,** 4971-4977 (2010).
643 19. Zhang, G. *et al*. Cell-based screen for discovering lipopolysaccharide biogenesis inhibitors. *Proc. Natl. Acad.*
644 *Sci. U.S.A.* **115,** 6834-6839 (2018).
645 20. Fu, L., Wan, M., Zhang, S., Gao, L., Fang, W. Polymyxin B Loosens Lipopolysaccharide Bilayer but Stiffens
646 Phospholipid Bilayer. *Biophys. J*. **118,** 138-150 (2020).
647 21. Liu, Y. Y. *et al*. Emergence of plasmid-mediated colistin resistance mechanism MCR-1 in animals and human
648 beings in China: a microbiological and molecular biological study. *Lancet Infect. Dis*. **16,** 161-168 (2016).
649 22. Carroll, L. M. *et al.* Identification of Novel Mobilized Colistin Resistance Gene *mcr-9* in a Multidrug-Resistant,
650 Colistin-Susceptible *Salmonella enterica* Serotype Typhimurium Isolate. *MBio.* **10,** e00853-19 (2019).
651 23. Nang, S. C., Li, J., Velkov, T. The rise and spread of *mcr* plasmid-mediated polymyxin resistance. *Crit. Rev.*
652 *Microbiol.* **45,** 131-161 (2019).
653 24. Skov, R. L., Monnet, D. L. Plasmid-mediated colistin resistance (*mcr*-1 gene): three months later, the story
654 unfolds. *Euro. Surveill.* **21,** 30155 (2016).
655 25. Wang, C. *et al*. Identification of novel mobile colistin resistance gene *mcr-10*. *Emerg. Microbes Infect*. **9,** 508-
656 516 (2020).
657 26. Raetz, C. R., Reynolds, C. M., Trent, M. S., Bishop, R. E. Lipid A modification systems in gram-negative
658 bacteria. *Annu. Rev. Biochem*. **76,** 295-329 (2007).
659 27. Simpson, B. W., Trent, M. S. Pushing the envelope: LPS modifications and their consequences. *Nat. Rev.*
660 *Microbiol.* **17,** 403-416 (2019).
661 28. Okuda, S., Sherman, D. J., Silhavy, T. J., Ruiz, N., Kahne, D. Lipopolysaccharide transport and assembly at the
662 outer membrane: the PEZ model. *Nat. Rev. Microbiol*. **14,** 337-345 (2016).
663 29. Zhou, Z., White, K. A., Polissi, A., Georgopoulos, C., Raetz, C. R. Function of *Escherichia coli* MsbA, an
664 essential ABC family transporter, in lipid A and phospholipid biosynthesis. *J. Biol. Chem*. **273,** 12466-12475
665 (1998).
666 30. Li, Y., Orlando, B. J., Liao, M. Structural basis of lipopolysaccharide extraction by the $LptB_2FGC$ complex.
667 *Nature*. **567,** 486-490 (2019).
668 31. Poirel, L., Jayol, A., Nordmann, P. Polymyxins: Antibacterial Activity, Susceptibility Testing, and Resistance
669 Mechanisms Encoded by Plasmids or Chromosomes. *Clin. Microbiol. Rev*. **30,** 557-596 (2017).
670 32. Janssen, A. B. *et al*. Nonclonal Emergence of Colistin Resistance Associated with Mutations in the BasRS
671 Two-Component System in *Escherichia coli* Bloodstream Isolates. *mSphere.* **5,** e00143-20 (2020).

672 33. Brennan-Krohn, T., Pironti, A., Kirby, J.E. Synergistic Activity of Colistin-Containing Combinations against
673 Colistin-Resistant Enterobacteriaceae. *Antimicrob. Agents Chemother*. **62,** e00873-18 (2018).
674 34. Dortet, L. *et al.* Rapid detection and discrimination of chromosome- and MCR-plasmid-mediated resistance
675 to polymyxins by MALDI-TOF MS in *Escherichia coli*: the MALDIxin test. *J. Antimicrob. Chemother.* **73,** 3359-
676 3367 (2018).
677 35. Weiss, R. L., Fraser, D. Surface Structure of Intact Cells and Spheroplasts of *Pseudomonas aeruginosa*. *J.*
678 *Bacteriol.* **113,** 963-968 (1973).
679 36. Furniss, R. C. D. *et al.* Detection of Colistin Resistance in *Escherichia coli* by Use of the MALDI Biotyper Sirius
680 Mass Spectrometry System. *J. Clin. Microbiol.* **57,** e01427-19 (2019).
681 37. Helander, I. M., Mattila-Sandholm, T. Fluorometric assessment of gram-negative bacterial permeabilization.
682 *J. Appl. Microbiol.* **88,** 213-219 (2000).
683 38. Allison, D. G., Lambert, P. A. Modes of Action of Antibacterial Agents. *Molecular Medical Microbiology.* 583-
684 598 (2015).
685 39. Pietschmann, S., Hoffmann, K., Voget, M., Pison, U. Synergistic effects of miconazole and polymyxin B on
686 microbial pathogens. *Vet. Res. Commun*. **33,** 489-505 (2009).
687 40. Taylor, S.D., Palmer, M. The action mechanism of daptomycin. *Bioorg. Med. Chem*. **24,** 6253-6268 (2016).
688 41. Zendo, T., Yoneyama, F., Sonomoto, K. Lactococcal membrane-permeabilizing antimicrobial peptides. *Appl.*
689 *Microbiol. Biotechnol*. **88,** 1-9 (2010).
690 42. Osborn, M. J., Gander, J. E., Parisi, E., Carson, J. Mechanism of assembly of the outer membrane of
691 *Salmonella typhimurium*. Isolation and characterization of cytoplasmic and outer membrane. *J. Biol. Chem.*
692 **247,** 3962-3972 (1972).
693 43. Yamato, I., Anraku, Y., Hirosawa, K. Cytoplasmic membrane vesicles of *Escherichia coli*. A simple method for
694 preparing the cytoplasmic and outer membranes. *J. Biochem*. **77,** 705-18 (1975).
695 44. Moore, R. A., Hancock, R. E. Involvement of outer membrane of *Pseudomonas cepacia* in aminoglycoside
696 and polymyxin resistance. *Antimicrob. Agents Chemother*. **30,** 923-926 (1986).
697 45. D'Amato, R. F., Thornsberry, C., Baker, C. N., Kirven, L. A. Effect of Calcium and Magnesium Ions on the
698 Susceptibility of *Pseudomonas* Species to Tetracycline, Gentamicin Polymyxin B, and Carbenicillin.
699 *Antimicrob. Agents Chemother*. **7,** 596-600 (1975).
700 46. Andolina, G. *et al*. A Peptidomimetic Antibiotic Interacts with the Periplasmic Domain of LptD from
701 *Pseudomonas aeruginosa*. *ACS Chem. Biol*. **13,** 666-675 (2018).
702 47. Sperandeo, P. *et al.* Functional Analysis of the Protein Machinery Required for Transport of
703 Lipopolysaccharide to the Outer Membrane of *Escherichia coli*. *J. Bacteriol.* **190,** 4460-4469 (2008).
704 48. Odds, F. C. Synergy, antagonism, and what the chequerboard puts between them. *J. Antimicrob. Chemother*.
705 **52,** 1 (2003).

706 49. Hoppe Parr, K. A. *et al*. Modification of sample processing for the Limulus amebocyte lysate assay enhances
707 detection of inflammogenic endotoxin in intact bacteria and organic dust. *Innate Immun*. **23,** 307-318
708 (2017).
709 50. Takayama, K. *et al*. Influence of fine structure of lipid A on Limulus amebocyte lysate clotting and toxic
710 activities. *Infect Immun* **45,** 350-355 (1984).
711 51. Bernardini F., Dale G. E., Wach A., Obrecht D., WS01-4 Pharmacokinetics and pharmacodynamics of
712 murepavadin (POL7080) in neutropenic lung infection models when evaluated by aerosol administration. *J.*
713 *Cyst Fibrosis*. **18,** S2 (2019).
714 52. Yapa, S. W. S. *et al.* Pulmonary and systemic pharmacokinetics of inhaled and intravenous colistin
715 methanesulfonate in cystic fibrosis patients: targeting advantage of inhalational administration. *Antimicrob.*
716 *Agents Chemother*. **58,** 2570-9 (2014).
717 53. Melchers, M. J. *et al.* Pharmacokinetics and Pharmacodynamics of Murepavadin in Neutropenic Mouse
718 Models. *Antimicrob. Agents Chemother*. **63,** e01699-18 (2019).
719 54. Aoki, N. *et al.* Efficacy of colistin combination therapy in a mouse model of pneumonia caused by multidrug-
720 resistant *Pseudomonas aeruginosa. J. Antimicrob. Chemother.* **63,** 534-542 (2009).
721 55. Lehman, K. M., Grabowicz, M. Countering Gram-Negative Antibiotic Resistance: Recent Progress in
722 Disrupting the Outer Membrane with Novel Therapeutics. *Antibiotics*. **8,** E163 (2019).
723 56. Wiegand, I., Hilpert, K., Hancock, R. E. Agar and broth dilution methods to determine the minimal inhibitory
724 concentration (MIC) of antimicrobial substances. *Nat. Protoc.* **3,** 163-175 (2008).
725 57. Loh, L. N., Ward, T. H. *Escherichia coli* K1 invasion of human brain microvascular endothelial cells. *Methods*
726 *Enzymol.* **506,** 93-113 (2012).
727 58. Lam, J. S., Anderson, E. M., Hao, Y. LPS quantitation procedures. *Methods Mol. Biol*. **1149,** 375-402 (2014).
728 59. Clarke, T. B. Early innate immunity to bacterial infection in the lung is regulated systemically by the
729 commensal microbiota via nod-like receptor ligands. *Infect. Immun.* **82,** 4596-4606 (2014).
730 60. Brown, R. L., Sequeira, R. P., Clarke, T. B. The microbiota protects against respiratory infection via GM-CSF
731 signaling. *Nat. Commun.* **8,** 1512 (2017).
732 61. Lee, D. G. *et al.* Genomic analysis reveals that *Pseudomonas aeruginosa* virulence is combinatorial. *Genome*
733 *Biol.* **7,** (2006).
734